Wheat gluten/LDPE based thermoplastic vulcanizates containing LDPE-g-MA as compatibilizer

L. Telen[a], K. J. A. Jansens[b,e], I. Verpoest[c,f], J. A. Delcour[b,e], P. Van Puyvelde[d,f], B. Goderis[a,e,f]

[a] *Polymer Chemistry and Materials Division, KU Leuven, Chemistry Department, Celestijnenlaan 200F, B-3001 Leuven, Belgium*

[b] *Laboratory of Food Chemistry and Biochemistry, KU Leuven, Kasteelpark Arenberg 20, B-3001 Leuven, Belgium*

[c] *Department of Materials Engineering, KU Leuven, Kasteelpark Arenberg 44, B-3001 Leuven, Belgium*

[d] *Department of Chemical Engineering, Applied Rheology and Polymer Processing, KU Leuven, Willem de Croylaan 46, B-3001 Leuven, Belgium*

[e] *Leuven Food Science and Nutrition Research Centre (LFoRCe), KU Leuven*

[f] *Leuven Material Research Centre (Leuven-MRC), KU Leuven*

Abstract

Traditionally, thermosetting wheat gluten based rubbers are produced from a glycerol plasticized gluten rubber precursor which spontaneously crosslinks during high temperature molding. We prepared thermoplastic elastomers by extruding the gluten rubber precursor at high temperature in presence of low density polyethylene (LDPE) to which maleic anhydride grafted LDPE (LDPE-g-MA) was added. At a proper LDPE/LDPE-g-MA ratio the desired phase-separated thermoplastic vulcanisate (TPV) morphology was obtained which consisted of finely dispersed gluten rubber particles, covalently anchored to the thermoplastic matrix. The TPVs with rubber contents up to 70 wt% can be injection molded multiple times without loss of performance. Interestingly, the water absorption of the TPVs is much lower than that of classical gluten rubber materials while the rubber elastic recovery is maintained. The behavior in tensile testing was rationalized in terms of the TPV-typical heterogeneous, plastic deformation mechanism. The low strains at break were related to the presence of contaminants.

Corresponding author: bart.goderis@chem.kuleuven.be (B. Goderis)

Email addresses: lien.telen@chem.kuleuven.be (L. Telen), koen.jansens@biw.kuleuven.be (K.J.A. Jansens), ignaas.verpoest@mtm.kuleuven.be (I. Verpoest), jan.delcour@biw.kuleuven.be (J.A. Delcour), peter.vanpuyvelde@CIT.kuleuven.be (P. Van Puyvelde)

Keywords: thermoplastic vulcanizate, wheat gluten, mechanical properties

1. Introduction

A thermoplastic elastomer (TPE) combines the typical properties and functional performance of rubbers with the melt processability of thermoplastic polymers (Coran et al., 1981). A thermoplastic vulcanizate (TPV) is a TPE consisting of a fine dispersion of

rubbery particles embedded in a continuous thermoplastic matrix. TPVs are produced by the high temperature extrusion of a rubber precursor in the presence of a thermoplastic polymer (Gessler and Haslett, 1962). In this process, the rubber precursor is dynamically crosslinked (vulcanized) (AbdouSabet et al., 1996). The associated viscosity increase together with the applied shear forces are crucial for the material phase morphology development. In contrast to traditional thermoset rubbers, TPVs and TPEs are recyclable. However, even if large scale after-use recycling is not manageable, their thermoplastic character is advantageous as it e.g. allows for the recuperation of production scrap. Current commercial TPVs consist of polypropylene matrices and dynamically vulcanized ethylene propylene diene monomer (EPDM) rubber particles. The blends often contain extender oils, crosslinking (co)agents and occasionally additives such as carbon black (Babu and Naskar, 2011).

Nowadays, considerable research is conducted towards bio-based plastics from renewable resources as alternatives for traditional petroleum based plastic (Babu et al., 2013). In this context and amongst other natural biopolymers, wheat gluten, the storage protein found in wheat kernels, has received attention (Bietz and Lookhart, 1996; Day et al., 2006). Wheat gluten typically ends up in food products such as bread (Delcour et al., 2012). However, being available in large quantities as a relatively cheap co-product of the starch industry, it also represents an annually renewable feedstock with great potential for the production of bioplastics, in particular because of its unique viscoelastic behavior and ability to spontaneously crosslink at high temperature (Lagrain et al., 2010). For some non-food applications the rapid biodegradability of wheat gluten can also be an advantage (Domenek et al., 2004).

Gluten can be divided into two protein classes: gliadins and glutenins. Gliadins are single chained polypeptides with a molecular weight ranging from 30 000 to 80 000 g/mol. They are extractable in aqueous alcohol and all of their cysteine residues are involved in intramolecular disulfide bonds. Glutenins, on the other hand, are unextractable in aqueous alcohol and are composed of glutenin subunits, connected through intermolecular disulfide bonds. This chain connectivity results in a molecular weight ranging from 80 000 to several million g/mol. In addition to intermolecular disulfide bonds, glutenins also contain intramolecular disulfide bonds and free sulfhydryl functionalities (Delcour et al., 2012).

During heat treatment, the oxidation of free sulfhydryl groups and sulfhydryl-disulfide interchange reactions create disulfide crosslinks that transform the biopolymer into a three-dimensional network (Redl et al., 2003; Sun et al., 2007). In the presence of high amounts of plasticizer (typically 30 wt%) a rubber is obtained. Several plasticizers can be used (Pommet et al., 2005) with glycerol, a co-product of the biodiesel production, being an interesting biobased option. With 30 wt% glycerol, the rubber at room temperature can be stretched to more than twice its original length. At very low temperatures, the material is a glass, which devitrifies typically around -50 °C (Sun et al., 2008a). Wheat gluten rubbers prepared via this recipe are commercialized by Tereos Syral under the trade name Meriplast®. Unfortunately, such materials suffer from water sorption and plasticizer leaching. Furthermore, since such materials are fully crosslinked, they cannot be recycled.

However, the natural tendency of gluten to crosslink at high temperature makes it an ideal candidate for conversion into TPV materials by high temperature extrusion in presence of a

plasticizer and a thermoplastic component. Since in TPV materials the rubber particles are embedded in a (hydrophobic) thermoplastic matrix, the rubber particles are shielded from water uptake and plasticizer leakage in addition to being thermoplastic. For manufacturing TPVs from wheat gluten, thermoplastic matrices should be selected with a melting point well below the gluten degradation temperature, say below 150 °C (Jansens et al., 2011). The thermoplastic component should also be immiscible with the gluten rubber phase. From this perspective, low density polyethylene (LDPE) can serve as thermoplastic matrix. However, to control the TPV morphology and to induce TPV specific mechanical behavior, a reduced surface tension and a strong interfacial adhesion between the rubber droplets and thermoplastic matrix is mandatory (Boyce et al., 2001a). For LDPE in combination with a gluten based rubber this can be achieved by using a maleic anhydride (MA) grafted LDPE (LDPE-g-MA) (Borah and Chaki, 2011; Jiang et al., 2003; Moly et al., 2006). Such MA functionalities have been successful in the compatibilization of immiscible blends of polyolefins and polyamides (Jiang et al., 2003) and were e.g. also used in the manufacturing of TPV materials based on polyamide 6 and EPDM rubber (Oderkerk et al., 2002). MA can react with the amine end-group, the in-chain peptide linkages or the side-chain amide groups of several amino acid residues such as asparagine (Asn) and glutamine (Gln). The Asp/Asn and Glu/Gln concentration in gluten respectively equals 2.8 mole% and 31.9 mole% (Rombouts et al., 2009) and according to Delcour and Hoseney (2010), the Glu/Gln share can almost fully be attributed to Gln. Compatibilizing reactions are also possible with lysine (Lys, 1.4 mole%), serine (Ser, 5.7 mole%), threonine (Thr, 2.8 mole%) and thyrosine (Tyr, 2.8 mole%). Commercial wheat gluten typically contains between 7% and 16% starch (Van Der Borght et al., 2005).

This work reports on the manufacturing and properties of wheat gluten based TPV materials with LDPE as thermoplastic matrix. Maleic anhydride grafted LDPE (LDPE-g-MA) and blends of LDPE and LDPE-g-MA were used as well. By varying the blend composition, the amount of compatibilizing agent was varied systematically. The properties of the obtained TPV materials are compared to those of the pure gluten rubber and LDPE phases. TPVs were produced from gluten as a whole or from a gliadin enriched fraction.

It will be demonstrated that recyclable, wheat gluten based thermoplastic elastomers can be made with a reduced tendency to absorb water and with elastomeric properties comparable to those of existing, medium hard, thermosetting gluten based rubbers.

2. Experimental section

2.1 Sample preparation

Gluten powder, 77.8% protein based on dry weight (db), 10.6% (db) starch and 7.3% (db) of lipids was obtained from Tereos Syral, Aalst, Belgium. Gliadin and glutenin enriched fractions were prepared from gluten by first extracting (shaking 1hour, 150rpm) gluten powder (20.0g) three times in 60/40 ethanol/water (v/v). After each extraction step, samples were centrifuged (10 min, 10 000 g) and the supernatants were pooled. After evaporation of the ethanol from the supernatants (Rotavapor R3000, Büchi, Flawil, Switzerland) and freeze drying, the sample was ground (laboratory mill, IKA, Staufen, Germany) and sieved (250 μm). The obtained powder is referred to as the gliadin enriched

fraction. The water content was adjusted back to equilibrium moisture content by adding the appropriate amount of crushed ice.

Gluten and its gliadin enriched fraction were converted into rubber precursors by mixing them with 30 wt% of glycerol (Acros Organics, 99.5%) first gently by hand and then by extruding at 60 °C for 5 min at 100 rotations per minute (rpm) under N_2-atmosphere using a co-rotating fully intermeshing recirculating midi twin screw extruder of 15 cm^3 (DSM Xplore, Geleen, The Netherlands). The addition of 30 wt% glycerol was a compromise to achieve maximum plasticization without glycerol leaching. All extrusion steps mentioned further below were with the same extruder under N_2-atmosphere.

The LDPE-g-MA powder (Sigma-Aldrich, St. Louis, MO, USA, 456632) (T_m of 105 °C) was pre-extruded at 130°C and converted into pellets to facilitate feeding during actual TPV manufacturing. The LDPE-g-MA has a saponification number of 32-36 mg KOH/g. Since for every MA residue, 2 KOH equivalents are needed, this corresponds to approximately 1 ethylene out of 100 being grafted with MA (0.85-0.92 mole%). Alternatively, the LDPE-g-MA content can be expressed in terms of wt% MA, this is 2.8-3.1 wt% MA. LDPE (Sigma-Aldrich, 428043) (T_m of 116 °C) was purchased in pellet form.

For manufacturing the TPVs, the thermoplastic components were first fed to the extruder at 130°C. The LDPE and pre-extruded LDPE-g-MA were melted, pure or as a blend according to the following LDPE/LDPE-g-MA ratio's: 100/0, 75/25, 50/50, 25/75 or 0/100. Once the thermoplastic matrix was in the molten state the rubber precursor was added and blending was allowed for 5 min. Variations were made in the rotation speed (50, 100 or 150 rpm), the rubber/thermoplast ratio (50/50, 60/40, 70/30) and the protein component (gluten as a whole or the gliadin fraction).

The TPV extrudate was injection molded into standardized dumbbell shaped tensile bars (90 mm, 30 mm gauche length X 4.8 mm X 1.5 mm) with a micro-injection molding machine (DSM) having a barrel capacity of 2.45 cm^3. This was accomplished with the reservoir at 130 °C, the mold at 40 °C and using a pressure of 2.5 bar. Samples of the pure thermoplastic component were prepared in exactly the same way. For pure rubber specimen another route had to be followed since putting the precursor at 130 °C resulted in excessive crosslinking, preventing injection molding. Instead, the rubber precursor was heated up to 100 °C in the reservoir and injected in the mold at 130°C using a pressure of 2.5 bar. Next, the material was left inside the mold to crosslink for 5 min, thereby simulating the TPV extrusion step as closely as possible. For characterizing the melt miscibility of the thermoplastic blend components (see section 3.2), the extruded LDPE/LDPE-g-MA blends were also compression molded using a manual, two-column hydraulic laboratory press (model M, Carver, Inc., Wabash, IN, USA) at 130°C for 6 min with a pressure of 10.34 MPa (1500psi). The material was covered with Teflon sheets to facilitate mold release after cooling the material rapidly to room temperature.

2.2 Molecular characterization

As a starting point for the molecular characterization, all samples (1.0 mg protein/ml) were extracted with a sodium phosphate buffer (0.05 M, pH 6.8) containing 2.0% (w/v) sodium dodecyl sulfate (SDS, Acros Organics, Geel, Belgium) as described by Jansens et. al. (2011). Prior to exposing the injection molded samples to the SDS containing medium, the materials

were ground under cryogenic conditions and sieved (250 µm). The level of SDS extractable protein (SDSEP) reflects the portion of protein that is not crosslinked to such a degree that it cannot be extracted in the SDS containing medium.

To evaluate the SDSEP content under reducing conditions, samples (1.0 mg protein/ml) were extracted under nitrogen atmosphere with the same buffer additionally containing 1.0% (w/v) dithiothreitol (DTT, Acros Organics) and 2.0 M urea. The level of SDSEP under reducing conditions (SDSEPred) reflects the amount of protein that is either not crosslinked or crosslinked via (reducible) disulfide bridges. The remaining non-extractable fraction reflects the amount of protein crosslinked via non-reducible covalent bonds, such as e.g. isopeptide bonds (Jansens et al., 2011). All extractions were performed in triplicate. After centrifugation (10 min, 10000 g) and filtration on polyethersulfone (0.45 µm, Millex-HP, Millipore, Carrigtwohill, Ireland), extracted proteins were separated with size exclusion high pressure liquid chromatography (SE-HPLC) as described by Lagrain et al. (2005) using a LC-2010HT system (Shimadzu, Kyoto, Japan) with automatic injection. The extracts (60 µl) were loaded on a BioSep SEC-S4000 column (300 x 7.8 mm, Phenomenex, Torrance, CA, USA) and eluted with acetonitrile (ACN)/water (1:1, v/v) containing 0.05% (v/v) trifluoroacetic acid (TFA). The flow rate was 1.0 ml/min at a temperature of 30 °C (Veraverbeke and Delcour, 2002). Eluted protein was detected at 214 nm.

The elution profiles of unreduced samples were divided into two fractions using the lowest absorbance value between the two peaks as cutoff point, i.e. at an elution time of 7.2 min under the current conditions. The fractions containing higher and lower molecular weight proteins are referred to as the SDS extractable glutenin and SDS extractable gliadin, respectively. SDS extractable gliadin and SDS extractable glutenin levels were calculated from the corresponding peak areas and expressed as a percentage of the complete peak area of unmolded gluten when extracted under reducing conditions. The latter represents a maximum possible value for the SDSEP; i.e. the value corresponding to a complete extractable protein. Reported SDSEP values are also expressed in terms of such percentage.

The rubber crosslinking degree was also characterized using swelling experiments. In the case of TPV materials, such experiments also reveal information on the sample morphology as outlined in the discussion section. Swelling experiments were performed at 20°C by placing rectangular samples (20 X 10 X 1.50 mm) in water containing 20 mg/l sodium azide to avoid microbial growth. At regular time intervals, the sample mass was measured after having been removed from the container and removal of excess water with blotting paper.

Differences in molecular weight between LDPE and LDPE-g-MA were addressed qualitatively by measuring the shear rate dependent melt viscosity at 140°C. For LDPE-g-MA a stress controlled (AR 2000, TA Instruments, DE, USA) and for the LDPE a strain-controlled (ARES LS, TA Instruments) rheometer was used because of the lower viscosity of the former. Experiments were performed on 25 mm diameter discs, using a 1 mm gap in a parallel plate geometry. Shear rate sweeps were conducted in a range from 0.01 s^{-1} to 10 s^{-1}.

2.3 Morphological characterization

The material morphology was visualized using a XL30 FEG scanning electron microscope (SEM, Phillips, Eindhoven, The Netherlands). After cutting at room temperature with a razor, after fracture by tensile testing or after cold fracturing in liquid N_2 the exposed

internal surfaces were Au/Pd sputter coated to prevent electrostatic charge build-up during SEM visualization using an electron beam voltage of 10 keV and a secondary electron detector. SEM images of razor cut samples were contrast enhanced using standard image analysis software to better visualize the phases of interest.

Small angle X-ray scattering (SAXS) measurements were performed on a selection of samples with an XeuSS X-ray camera (Xenocs, Sassenage, France), comprising a GeniX 3D Molybdenum ultra-low divergence X-ray beam delivery system (wavelength λ = 0.71 Å) at a power of 50 kV–1 mA, a collimating assembly based on scatterless slits, a sample stage, a He flushed flight tube and a Mar345 image plate detector (MAR research, Norderstedt, Germany). The scattering angles were calibrated using silver behenate and expressed in terms of q, with $q = (4\pi\sin\theta)/\lambda$ and θ being half the scattering angle.

2.4 Mechanical characterization

The injection molded tensile bars were tested using an Instron (Norwood, MA, USA) 5985 tensile tester (1kN force cell) at 10 mm/min up to sample fracture. Initial sample width and thickness were measured using a caliper. The initial grip separation was 37mm for all experiments. A speckle pattern was spray painted on the sample. During deformation a camera (Limes, Messtechnik und Software GmbH, Krefeld, Germany) took pictures every 0.5 s. The axial strain developed during deformation was obtained using a digital image correlation algorithm (VIC-2D software, Correlated Solutions, Inc., SC, USA) using a subset of 23 and a step size of 3, working incrementally. The mechanical properties were calculated based on the strain averaged over the entire sample area, omitting the areas that were less than 1.5 times the width away from the clamps.

Engineering strain and stress at break were defined as the maximum values just before fracture. The modulus was extracted from the slope in the engineering stress-strain data between 0% and 2% strain for all materials except for the gluten and gliadin based rubbers for which the data below 1% strain were used as a non-linear stress-strain behavior was observed already at low strains for those materials. The area enclosed by the engineering stress-strain curve was taken as value for the material toughness. All measurements were performed at least in triplicate and average values with their standard deviations are reported.

The strain recovery behavior after tensile deformation was studied using the same set-up. The samples were deformed to a clamp displacement of 6 mm at 10 mm/min, which corresponds to approximately 10-15% strain. The stress while inverting the strain direction at 1 mm/min was measured down to a zero engineering stress. The recovery was calculated as 1 minus the ratio of the strain upon reaching zero stress and the maximum strain prior to inversion of the strain direction.

The shore D hardness was determined using a Shore D durometer (Zwick, Venlo, The Netherlands) as described in ISO 7619-1. The indentation time was 15s. Samples were 62 X 9.7 X 3.2 mm in size. Therefore 2 samples were placed on top of each other in order to reach the minimal thickness of 6 mm.

2.5 Thermal characterization

Differential scanning calorimetery (DSC) heating, cooling and second heating runs were recorded at 10°C/min using a TA Instruments (New Castle, DE, USA) Q2000 heat-flux DSC, calibrated with an Indium standard. Five minutes of isothermal waiting time were allowed between the heating and cooling segments. Measurements were conducted between -30°C and 130°C. After subtracting an empty pan measurement and normalization to the sample mass and heating rate, data were obtained in units of specific heat capacity. The polyethylene crystallinities obtained from the first and second heating at 10°C/min of the pure thermoplastic components and of the polyethylene fraction within the TPV materials was determined at 25°C by integrating the area enclosed between the polyethylene melting peak and the curve extrapolated from the melt heat capacity signal (Mathot, 1994). This area was normalized to the theoretical heat of fusion of pure crystalline polyethylene at 25°C, i.e. 250J/g (Mathot, 1984). For the TPV materials, this value was further normalized to the mass fraction polyethylene in the material.

Thermo gravimetrical analysis (TGA) was performed using a TGA 2950 (TA Instruments) under nitrogen atmosphere (60mL/min) while heating at 2°C/min from room temperature to 550°C.

3. Results and discussion

This section starts with a discussion on the gluten rubber characteristics and is followed by a section on the pure thermoplastic matrix properties. These data are indispensable for an adequate discussion of the properties of the actual TPV materials in the final part.

3.1 Gluten rubber

Gluten powder was converted into a rubber precursor by adding 30wt% of glycerol and extruding at 60°C. The SDSEP of the received gluten powder was 81%. Extrusion at 60 °C for 5 min in the presence of glycerol decreased the SDSEP to 62%, indicating partial crosslinking. Figure 1 shows the SE-HPLC profiles of the gluten powder and the extruded rubber precursor extracted with SDS containing medium. Comparison of both profiles demonstrates that the loss in extractability was higher for the glutenins (peak around 5.5 min) than for the gliadins (peak around 8 min). Increasing the extrusion time at 60 °C, decreased the extractability, with the glutenin fraction being affected most (data not shown). Clearly, the glutenins were incorporated preferentially into the non-extractable molecular network when using 60°C as extrusion temperature.

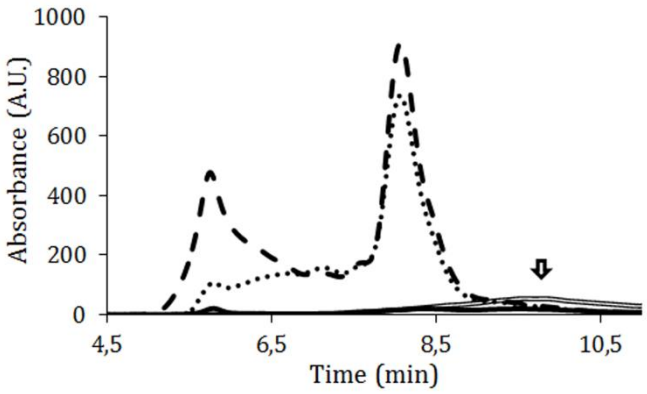

Fig. 1: SE-HPLC profile of gluten powder as received (dashed line), the rubber precursor extruded at 60 °C for 5 min at 100 rpm under nitrogen atmosphere (dotted line), the gluten rubber after injection molding at 130°C (full line) and the rubber extracted from an LDPE/LDPE-g-MA 75/25 based TPV containing 60 wt% of gluten rubber (full open line) extracted with SDS containing medium. The arrow highlights low molecular weight degradation products in the TPV material.

During extrusion, crosslinking is established as a result of the oxidation of free SH groups and disulfide-sulfhydryl interchange reactions (Fernandes and Ramos, 2004; Pommet et al., 2005; Schofield et al., 1983). Glutenins contain free SH groups that readily take part in crosslinking reactions. In contrast, gliadins do not have free SH groups and their intramolecular disulfide bonds are less accessible for disulfide exchange reactions since this requires full protein unfolding which, although starting at 55°C, is only fully accomplished above 75°C (Schofield et al., 1983). Irrespective of the extrusion time, SDSEPred is 100% for the precursor material extruded at 60 °C, indicating that disulfide bonds are the main responsible for the crosslinking, without significant contributions from non-reducible intermolecular crosslinks, such as isopeptide bonds.

After injection molding of the precursor at 130°C for 5 min minimal extractability (lower than 8%) was reached, as can be seen from the very small area below the curve of the SE-HPLC profile of the gluten rubber in Figure 1. Indeed, excessive crosslinking at 130°C transforms the gluten rubber precursor into a true rubber network. The SDSEPred of the injection molded rubber was 90%, pointing at the formation of some intermolecular crosslinks other than disulfide bonds. However, disulfide bonds remained most abundant.

TGA is well suited for rubber precursor and final rubber composition determination. The top panel in Figure 2 shows the TGA curve of the gluten powder after storage as it is used in all gluten rubber and TPV preparations. According to Sun et al. (2004), below 200 °C both free and bound water are released. Based on the TGA analysis by Gomez-Martinez et al. (2011), gluten protein volatilization starts from 200 °C onwards. Accordingly, the TGA profile was extrapolated by the constant value at 200°C down to 25°C. The difference between this extrapolated curve and the overall TGA curve is suggested to represent the water share in the TGA curve. It appears that at 25 °C 10.4 (±0.6) wt% water was present in the gluten powder. In the ramp up to 70 °C, about 7.1 wt% water was lost and above 150 °C the remaining fraction followed. The former is likely related to the free, the latter to the

bonded water (Domenek et al., 2004). The dashed and dotted lines in the top panel of Figure 2 respectively represent the dry gluten and water fractions in the gluten powder sample. This dry gluten profile can be scaled to match the gluten rubber TGA profile at the high temperature side (400 °C-540 °C), as illustrated in the bottom panel of Figure 2. By doing so, the rubber TGA profile is split into its dry gluten (dashed curve) and solvent (dotted line) shares. The solvent share combines the glycerol and the water fraction within the rubber. Interestingly, the sum of these fractions approached 36.6 wt%. A significant portion (35.8 wt%) of solvent could be found in the gluten rubber precursor, when treating its TGA profile in a similar way (data not shown). Given that 30 wt% glycerol was added to the gluten powder that contained 10.4 % water, no water or glycerol was lost during extrusion or injection molding. TGA experiments on pure glycerol, following the procedure by Castell et al. (2009), revealed that this liquid prior to mixing contained at most 0.5 wt% water.

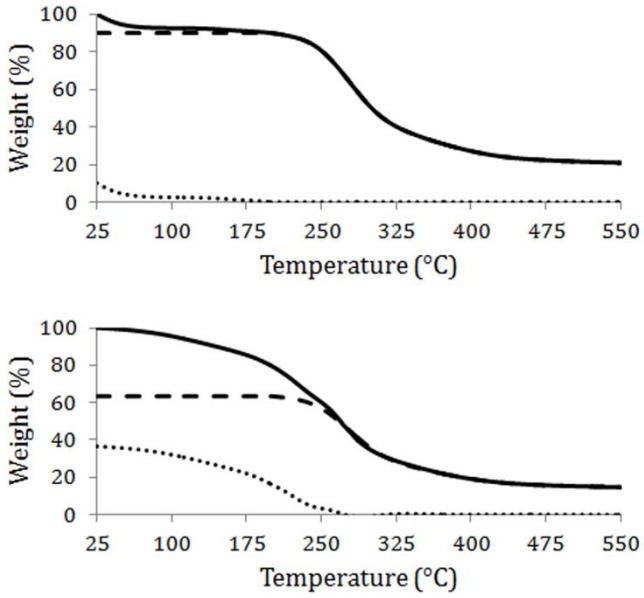

Fig. 2: TGA wt% as a function of temperature for the gluten powder (top panel) and the compression molded gluten rubber (bottom panel); The dry gluten shares are represented by dashed and the solvent shares by dotted curves.

The simple additive TGA analysis suggests that gluten pyrolysis under N_2 atmosphere does not depend on whether or not the gluten material is crosslinked or in contact with glycerol. In all cases (powder, rubber precursor or rubber), a residue was left at high temperature, equal to 20.1 (± 1.5) wt% of the dry gluten mass. On the other hand, a TGA experiment in air resulted in complete volatilization of the gluten powder by oxidative degradation (data not shown). Figure 2 furthermore revealed a continuous loss of glycerol/water between 25°C and 250°C, confirming earlier results (Gomez-Martinez et al., 2011). Plasticizer loss as well as protein degradation should be avoided during processing and everyday use of gluten based rubbers and TPVs. TGA experiments on TPV materials demonstrated that no plasticizer is lost during extrusion and injection molding at 130°C (see below).

Gluten protein degradation, however, starts prior to volatilization in TGA. Earlier SE-HPLC work revealed molecular weight reductions when exposing gluten to temperatures equal to or above 150°C (Jansens et al., 2011). Low molecular weight fragments could be seen in negligible amounts in the Figure 1 profiles, demonstrating that 130°C is suited for gluten rubber and TPV manufacturing.

Compression molded, unplasticized, rigid gluten material tends to take up as much as its own mass in water when submersed into it (Jansens et al., 2013). Plasticized gluten rubbers also take up large quantities of water when submersed, but do so very differently as demonstrated in Figure 3. Whereas the water uptake increases continuously up to saturation in rigid gluten materials, the water uptake by glycerol plasticized gluten rubbers surpasses a maximum mass gain of 60% prior to leveling off at a value of about 40%. Compared to the rubber, the unplasticized sample shows a slower mass gain but a higher final level. This difference in behavior can be explained by the presence of glycerol in the rubber sample. Glycerol is hygroscopic, enhancing the initial water uptake. After three hours, glycerol leaching overtakes the water uptake and an overall mass decrease is observed. The sample mass after swelling and subsequent drying at 130°C corresponds to 76% of the initial dry mass. About 80% of the glycerol thus had left the sample. The protein retention reflects extensive crosslinking. Clearly, the water uptake of gluten based rubber is substantial and limits its outdoor applicability.

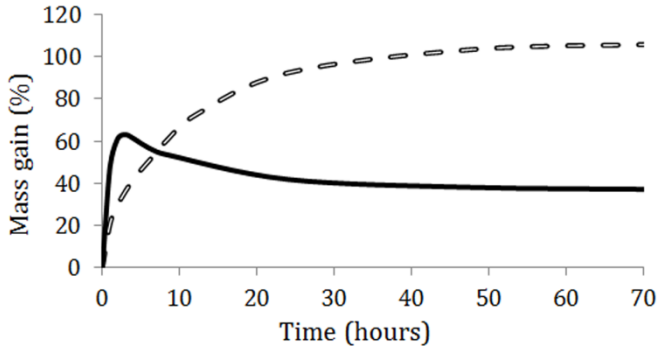

Fig. 3: Swelling behavior of injection molded gluten rubber (full curve) and unplasticized, rigid gluten material (dashed line). The rigid material was obtained by compression molding gluten powder with an initial moisture content of 5.6 wt% at 130 °C for 5 min (data adapted from (Jansens et al., 2013)).

The gluten rubber had a Young's modulus of 73 ± 14 MPa and an ultimate tensile stress and strain of 3.5 ± 0.2 MPa and 137 ± 18 % respectively. Compared to a typical vulcanized EPDM rubber, with an ultimate tensile strength of 2 MPa and an ultimate strain of about 300% (Wang et al., 2012), the gluten rubber was relatively stiff and less ductile. However, compared to other protein based rubbers such as rubbers from peas (Wang et al., 1996), the mechanical properties were comparable under identical humidity conditions. Note, however, that the mechanical properties of gluten rubber varied with the glycerol content and molding temperature (Domenek et al., 2004; Pommet at al., 2005). The shore D hardness of the gluten rubber equaled 19 ± 2, which classifies it as a medium hard rubber. Manufacturing rubbers from the glutenin enriched fraction was attempted but failed as extrusion at 60°C in presence of glycerol was not possible, likely due to the high glutenin

molecular weight and undesired crosslinking. Extrusion problems were not encountered for the gliadin fraction. Gliadin based rubbers had a lower modulus (56 ± 5 MPa), lower ultimate stress (2.3 ± 0.3 MPa) and higher ultimate tensile strain (170 ± 26 %) than rubbers based on complete gluten. The gliadin rubber toughness value (3.6± 1.0 MPa) was comparable to that of the gluten based rubber (4.4± 0.7 MPa).

It has been recognized that by altering the processing conditions an enhanced gliadin rubber performance can be obtained and high ultimate strains in particular (Sun et al., 2008b). No attempts were made to do so since the only relevant processing parameters in the present context are the ones that are as close as possible to those of the TPV materials.

Figure 4 shows SEM images of gluten or gliadin based rubber surfaces after cryo fracturing. The gliadin rubber surface (Figure 4B) was very smooth as expected for the brittle (cryo) fracture of glassy materials. The gluten rubber cryo fracture surface appeared layered, which points at shear yielding phenomena (Figure 4A). The rounded particles in the gluten rubber are starch granules, which do not adhere to the gluten matrix. The gliadin extraction process concentrates the starch in the solid fraction, and thus hardly any starch was present in the gliadin rubber.

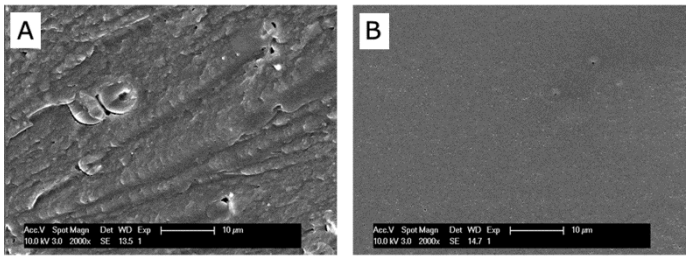

Fig. 4: SEM images of the fracture surface of a cryo-fractured gluten rubber sample (A) and a rubber prepared from gliadin rich fraction (B).

3.2 LDPE based thermoplastic component

LDPE was selected as thermoplastic matrix for manufacturing the TPV materials. To establish covalent crosslinks between the gluten rubber and LDPE phase, the addition of maleic anhydride grafted LDPE (LDPE-g-MA) was explored. The LDPE/LDPE-g-MA ratio was varied to contain 0, 25, 50, 75 or 100 wt% of LDPE-g-MA. Altering the LDPE/LDPE-g-MA ratio in blends of these components allowed addressing the effect of altering the MA content of the thermoplastic matrix on the TPV material morphology and properties. However, by blending, other relevant parameters such as the melt viscosity, (phase) morphology, crystallinity and mechanical properties were varied concomitantly.

MA grafting can decrease the molecular weight of the final product (Huang et al., 2006). Maintaining a reasonably high matrix viscosity (which is related to the matrix molecular weight) is crucial for establishing the desired TPV phase morphology (see section 3.3) (Huang et al., 2006). A value of 2200 Pa.s for the LDPE zero shear viscosity was obtained. According to the supplier, the LDPE-g-MA zero shear viscosity at 140°C falls in the range 1.7 to 4.5 Pa.s, which is about 3 decades lower than the LDPE value and thus indicative for a much lower LDPE-g-MA molecular weight. These values could not be confirmed since extrapolating to the LDPE-g-MA zero shear viscosity was not reliable because of

pronounced shear thinning. However, the viscosity at a shear rate of 1 s^{-1} was found to be 12.15 Pa.s for LDPE-g-MA and 1972 Pa.s for LDPE, which is in line with the zero shear rate values. In practice, the molecular weight decrease by maleation is often compensated for by adding non-maleated product (Huang et al., 2006). Blending LDPE to LDPE-g-MA thus also serves at elevating the matrix molecular weight.

Furthermore, the polarity introduced by maleation may induce incompatibility in the melt state when mixed with regular LDPE. According to Huang et al. (2006) ethylene/1-octene copolymers and their maleated counterparts are melt miscible provided the difference in maleation degree between the components is less than 0.9-1.25 MA wt% (Huang et al., 2006). Assuming a similar miscibility threshold for LDPE, the current LDPE-g-MA with an MA wt% of about 3 wt% should not be melt miscible with the LDPE. Huang et al. (2006), with advanced transmission electron microscopy and a special staining method, were able to visualize submicrometer sized spherical LDPE-g-MA droplets in demixed blends (Huang et al., 2006). A typical SEM image (Figure 5, part D) taken after compression molding and cold fracturing of an LDPE/LDPE-g-MA 75/25 blend revealed the presence of similar small globular entities, which are interpreted as LDPE-g-MA rich droplets, given that no such features were found in pure LDPE or LDPE-g-MA.

The submicrometer morphology of other compositions and of cryo-fractured injection molded blends was not clear. After all, the chemical and textural difference between the presumed phases should be very small and be readily obscured by fracture induced topological effects. When relying on the work by Huang et al. and on Figure 5 (part D), it is very plausible that the LDPE and LDPE-g-MA are not fully miscible.

Figure 5 also displays SEM images at lower magnification of cryo-fractured surfaces after injection molding. It shows fairly smooth LDPE (A) and LDPE-g-MA (C) surfaces in contrast to a more rough surface for the LDPE/LDPE-g-MA 75/25 blend (B).

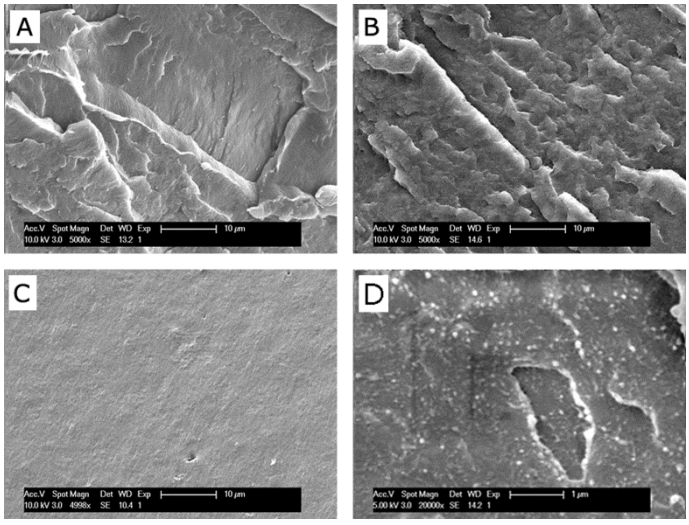

Fig. 5: SEM images of the fracture surface of a cryo-fractured LDPE (A), LDPE/LDPE-g-MA 75/25 (B) and LDPE-g-MA (C) manufactured by injection molding or the LDPE/LDPE-g-MA 75/25 blend manufactured by compression molding (D).

Blending different LDPE/LDPE-g-MA ratios may also affect the TPV properties by altering the thermoplastic matrix crystallinity. Figure 6 displays the crystallinities of the different LDPE/LDPE-g-MA blends from the DSCs first and second heating run. The LDPE crystallinity equaled approximately 45% and decreased with increasing LDPE-g-MA content down to about 30% for pure LDPE-g-MA.

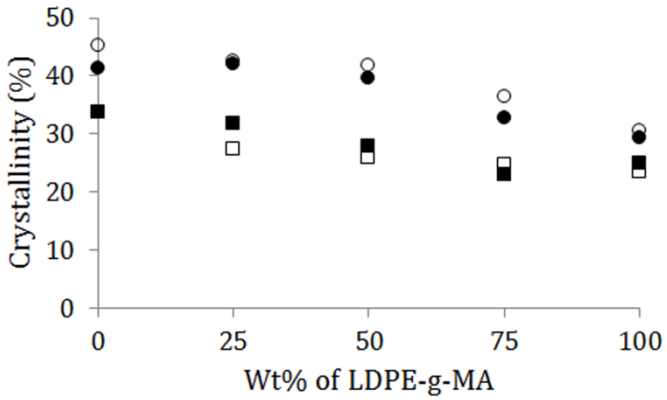

Fig. 6: Weight % crystallinity at 25 °C based on the first (full symbols) and second heating (open symbols) runs of the different injection molded LDPE/LDPE-g-MA blends (spheres) and corresponding TPVs materials with a gluten rubber content of 60 wt% (squares). For the TPV materials the crystallinity was normalized so that it represents the crystallinity in the LDPE/LDPE-g-MA matrices.

This crystallinity decrease was reflected in the gradual decrease of the modulus measured in a tensile test (Figure 7A). The stress at break followed a similar downward trend with increasing LDPE-g-MA content (Figure 7B). The engineering strain at break changed rather stepwise (Figure 7C). Pure LDPE-g-MA broke below 10% strain. Incorporating 25 wt% of LDPE resulted in an increase to about 35% but at higher LDPE levels the strain at break saturated at 100%. All LDPE/LDPE-g-MA samples at first deformed rather homogeneously. At strains of 10-15 % the strain rate locally accelerated by (faint) necking from which the strain further propagated through the entire material. Such a stage was never reached prior to failure for the pure LDPE-g-MA sample. The susceptibility to early failure reflected the inability of that polymer to delocalize local excess strain by strain hardening. The low ultimate strain for pure LDPE-g-MA and also for the 25/75 blend can be attributed to the low LDPE-g-MA molecular weight and the associated low entanglement density. Adding high molecular weight LDPE introduced the necessary entanglements and hence induced higher ultimate strains. The improvement leveled off at 50% LDPE and higher. Given that LDPE and LDPE-g-MA are not fully miscible, the changeover from LDPE-g-MA to LDPE typical ultimate strains may reflect a phase inversion with the LDPE-g-MA and LDPE rich phases being the matrix phases respectively below and above approximately 50wt% LDPE in the blend. The toughness values (Figure 7D) displayed a combined trend in which from LDPE to increasingly more LDPE-g-MA the toughness at first gently declined (mirroring the modulus and stress at break values) to rapidly drop beyond 50% LDPE-g-MA (just like the strain at break does).

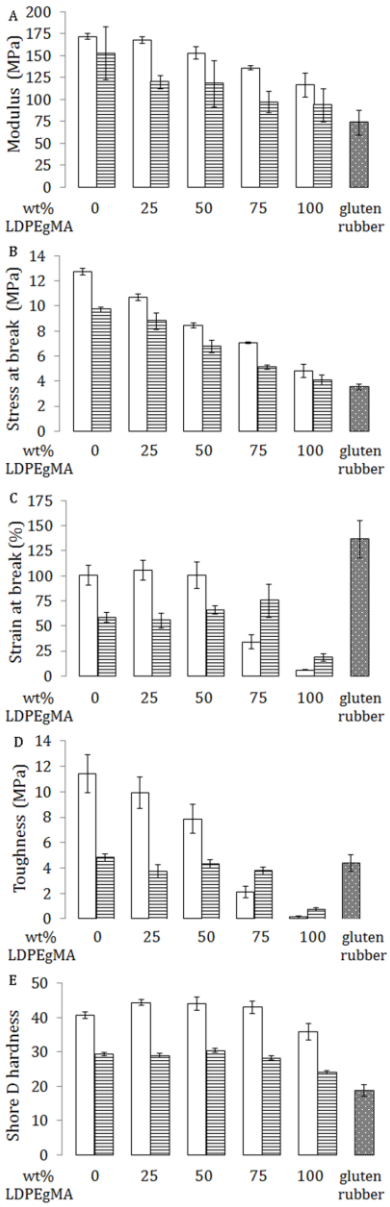

Fig. 7: Tensile test results and shore D hardness values of the LDPE/LDPE-g-MA blends (white bars) and the TPV materials based on 60 wt% gluten rubber and 40wt% of the different LDPE/LDPE-g-MA blends (horizontally dashed bars) as a function LDPE/LDPE-g-MA ratio (from left to right: 0/100, 75/25, 50/50, 25/75 and 100/0). For comparison, the values of pure gluten rubber were added. A: Young's modulus (MPa), B: stress at break (MPa), C: strain at break (%), D: toughness (MPa) and E: shore D hardness.

The decrease of the shore D hardness with increasing LDPE-g-MA content (Figure 7E) only manifested itself clearly at the highest LDPE-g-MA content and was thus less pronounced than that of the modulus, although the former was expected to qualitatively follow the latter (Qi et al., 2003). Besides crystallinity, also molecular orientation may have affected the compared parameters. The SAXS pattern in Figure 8A for the blend with 25 wt% of LDPE-g-

MA can be interpreted as a superposition of an isotropic ring with two meridional lobes. The lobes correspond to the scattering of lamellar stacks of which the normal is aligned parallel to the injection molding direction (Heeley et al., 2013). In absence of chain tilt, the observed crystal stack orientation reveals molecular orientation in the injection molding direction. The ring shaped scattering corresponds to a population of randomly oriented lamellar stacks and clearly contributes less to the SAXS pattern than the equatorial lobes. The intensity of the two contributions was, however, inverted in the SAXS pattern of the blend with 75 wt% of LDPE-g-MA (Figure 8B), revealing that random orientation dominated in this case. Apparently, the short LDPE-g-MA molecules rapidly relaxed prior to being frozen in the oriented state by crystallization, if they oriented at all. This was opposite to what happened in the LDPE fraction. Given that the molecular orientation ran parallel to the injection molding direction and parallel to the tensile testing direction, one could expect the modulus to be larger for higher degrees of molecular orientation. The direction of applied stress was perpendicular to the injection molding direction during the hardness test and therefore orientation effects were expected to contribute less. The decrease of the modulus with increasing LDPE-g-MA content was thus grounded in both a decrease of the crystallinity and of molecular orientation whereas the hardness values were primarily governed by the sample crystallinity.

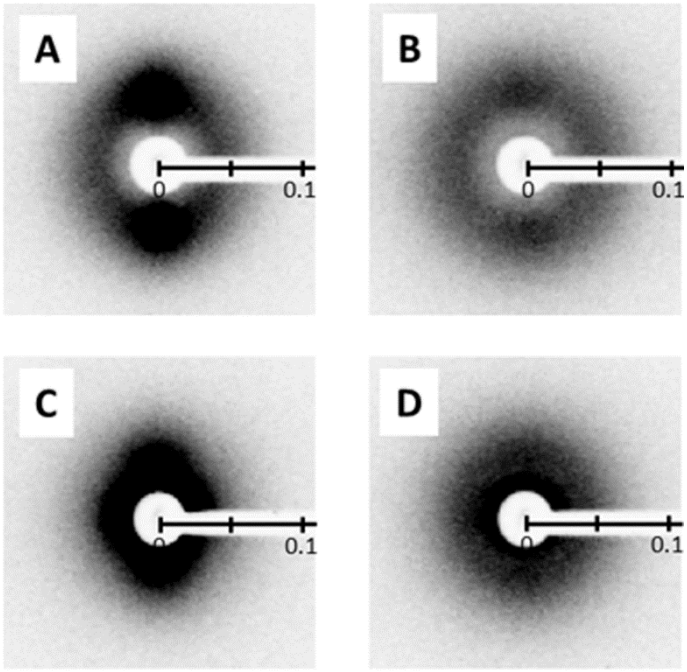

Fig. 8: Transmission SAXS patterns of samples with the injection molding direction positioned vertically for the 75/25 and 25/75 LDPE/LDPE-g-MA blends in respectively A and B and for the TPV materials with 60 wt% gluten rubber and 40 wt% 75/25 or 25/75 LDPE/LDPE-g-MA blends in C and D. The horizontal axis represents the scattering vector axis, q in $Å^{-1}$.

3.3 TPV materials

3.3.1 Influence of the component composition

TPV materials containing 60 wt% rubber and 40 wt% thermoplast were selected to evaluate the effects of altering the thermoplast LDPE/LDPE-g-MA ratio or the rubber precursor (gluten versus gliadin). The materials were compounded by extrusion for 5 min at 130 °C using 100 rpm under N_2 atmosphere and injection molded.

The melt phase morphology in immiscible polymer blends under flow is governed by the competition between the shear stress, which tends to deform dispersed phases and the interfacial tension, which tends to prevent this. Their ratio is called the capillary number, C_a, and is given by:

$$C_a = \frac{\dot{\gamma}\eta_m R}{\sigma_{12}} \qquad \text{(Equation 1)}$$

with the shear stress given by $\dot{\gamma}\eta_m$ and the interfacial tension by R/σ_{12}. The parameters $\dot{\gamma}$, η_m, R and σ_{12} represent the shear rate, the matrix viscosity, the characteristic radius of the dispersed phase and the interfacial tension between matrix and dispersed droplets (Taylor, 1932).

With all other parameters kept constant, R is expected to decrease during extrusion until C_a equals $C_{a,crit}$. At constant shear rate, smaller ultimate R values can be obtained by decreasing σ_{12} or by increasing η_m. Decreasing σ_{12} by adding LDPE-g-MA, however, goes together with a decrease of η_m. It follows that the overall effect of using LDPE-g-MA as matrix component is unclear. Another important parameter is p, the ratio of the particle viscosity over that of the matrix, η_p/η_m. Crace determined that $C_{a,crit}$ in the case of simple shear flow is the lowest when p is around 1 (Grace, 1982), implying that the finest dispersions can be achieved at p = 1. During dynamic crosslinking, p rapidly increases and above p = 3.5, particle break up is no longer possible (Grace, 1982). When the crosslinking reaction is too fast, particles may remain large or the system may get stuck in a co-continuous morphology, both of which are not desired for the TPV mechanical properties (l'Abee et al., 2010). Co-continuity is more relevant the higher the gluten rubber content is, even though the highly viscous rubber component has a tendency to form the dispersed phase (Utracki, 1990). The TPV phase morphology development during reactive extrusion is thus rather complex and should be in place prior to substantial rubber cross-linking which arrests the phase morphology development.

The sample morphology was studied by SEM on surfaces obtained by cutting at room temperature with a razor (Figure 9), after cryo-fracturing (Figure 10 A and B) and after tensile testing (Figure 10C and D). The gluten rubber phases in Figure 9 appear brighter because they are more electron rich and clearly decrease in size in going from the material based on pure LDPE-g-MA (Figure 9E) over the 25/75 and 50/50 blends (Figure 9D and 9C) to that based on the 75/25 LDPE/LDPE-g-MA blend (Figure 9B). In the latter case, gluten rubber particles are no longer visible at the displayed length scale. The lighter patches in this material in Figure 9B are topological artifacts, rather than a reflection of larger gluten rubber inclusions. Optical microscopy investigation confirms the absence of large rubber inclusion (data not shown). The system based on pure LDPE (Figure 9A) again exhibits larger gluten phases which very clearly are detached from the matrix by the action of

cutting. Figure 10 more clearly illustrates the larger rubber phases and their poor adhesion to the matrix. In Figure 10A, rather large phases are visible with interfaces loose from the matrix. The morphology is much finer and no interfacial detachments can be seen in the cryo-fractured surface of the system based on the 75/25 LDPE/LDPE-g-MA blend in Figure 10B. Furthermore, the rubber particles of the LDPE based system seem to have left the surface after tensile testing, suggesting that the large shell-like features in Figure 10C are the cavities where the rubber particles resided prior to tensile testing. Figure 10D shows no such features for the counterpart based on the 75/25 LDPE/LDPE-g-MA blend. The only loose particle in Figure 10C is a starch granule, which is larger than the gluten rubber particles, being approximately 2-3 μm across. Clearly, when no LDPE-g-MA is present, there is no interfacial bonding and σ_{12} must thus be large. Conversely, when only LDPE-g-MA is used, the interfaces are strong and hence σ_{12} must be small, but the reduced η_m lowers the shear stress such that a fine dispersion cannot be made. The stretched features in the Figures 9D and 9E even suggest co-continuity rather than a gluten rubber dispersion. The 75/25 LDPE/LDPE-g-MA blend matrix seems to have combined a low σ_{12} with a sufficiently high η_m and to have given rise to a strong interfacial bonding and the finest rubber dispersion of the systems studied. Note that in Figure 9 small holes are occasionally present also on the surfaces of the LDPE-g-MA containing samples. These are due to starch granules or fibrous wheat kernel contaminations that do not adhere well to the matrix or the gluten rubber. In this context it is relevant to mention an earlier report that LDPE-g-MA is not able to compatibilize starch with gluten (Bikiaris et al., 1998).

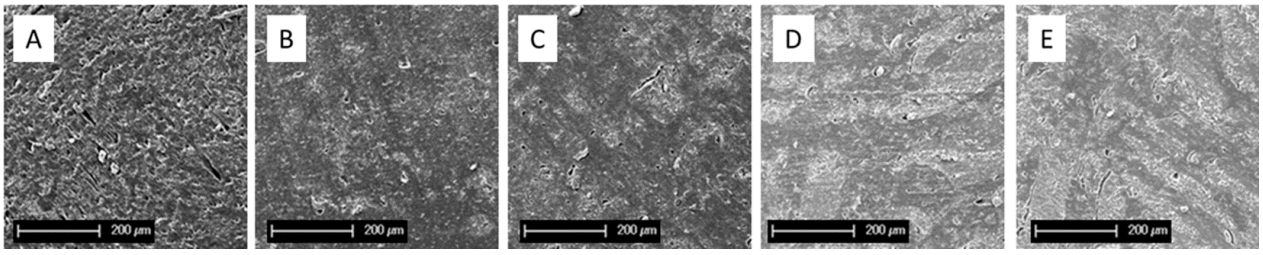

Fig. 9: SEM images of TPVs based on 60wt% gluten rubber and 40wt% LDPE/LDPE-g-MA with LDPE/LDPE-g-MA being 100/0 (A), 75/25 (B), 50/50 (C); 25/75 (D) and 0/100 (E). All samples were extruded at 100 rpm for 5 min. The surfaces were obtained by cutting at room temperature with a razor.

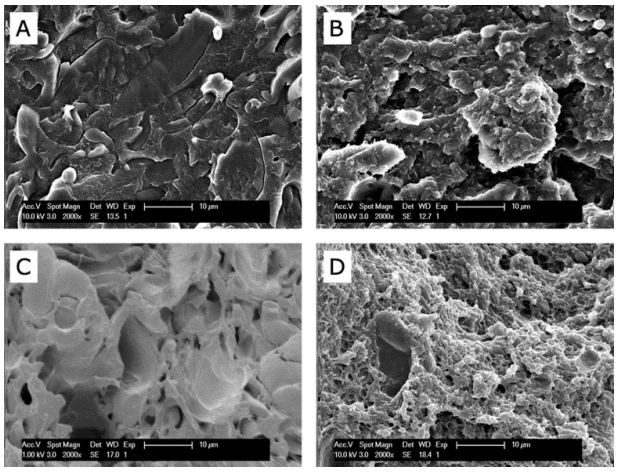

Fig. 10: SEM images of TPVs based on 60 wt% gluten rubber and 40 wt% LDPE/LDPE-g-MA with LDPE/LDPE-g-MA being 100/0 in (A) and (C) and 75/25 in (B) and (D). All samples were extruded at 100 rpm for 5 min. The surfaces were obtained by cryo-fracturing for (A) and (B) and are the fracture surfaces after tensile testing for (C) and (D).

The chromatogram in Figure 1A illustrates that the gluten rubber precursor actually converted into a crosslinked rubber during the TPV extrusion process. The SDSEP content of the TPV gluten rubber phases (area enclosed by the chromatogram) was as low as that of the pure rubber after injection molding at 130°C. However, the TPV chromatogram showed a small peak around 9.5 min, a signature of low molecular weight material, and thus indicating gluten degradation (Jansens et al., 2011). The degradation was probably too small to significantly affect the rubber properties in the TPV materials. Similar results were obtained irrespective of the matrix LDPE-g-MA content.

The TPV TGA profile displayed in Figure 11 (full line) was accurately reproduced by a proportional superposition of the TGA profiles of the pure gluten rubber (dashed line) and pure LDPE/LDPE-g-MA 75/25 thermoplastic component (dotted line). This simple additivity proves that the component ratios were preserved during extrusion and injection molding at 130°C. More specifically, no glycerol was lost.

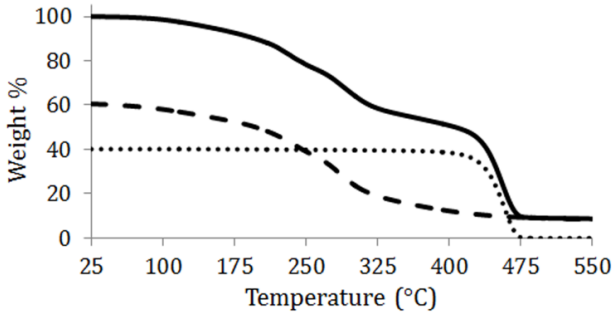

Fig. 11: TGA weight% of the TPV with 60% gluten rubber and 40% LDPE/LDPE-g-MA 75/25 (full line). The TGA profiles of the rubber (dashed line) and LDPE/LDPE-g-MA 75/25 (dotted line) fractions are scaled by multiplying by the TGA profiles of the pure components by respectively 0.6 and 0.4. The sum of the dashed and dotted profiles reproduces the TPV TGA profile.

Irrespective of the LDPE/LDPE-g-MA ratio, the TPV matrix crystallinity (Figure 6) was approximately 10% (absolute) lower than that of the pure LDPE/LDPE-g-MA materials. It seems that the rubber particles hindered the matrix crystallization. However, the DSC crystallization and melting peak temperatures of the thermoplastic TPV components were virtually identical to those of the corresponding pure LDPE/LDPE-g-MA blends (data not shown). The TPV SAXS patterns in Figure 8 did not reveal crystal orientation effects as clearly as for the pure components because of excess scattering at the smallest q-values, likely due to contributions from the gluten rubber-matrix morphology at a length scale larger than that of the semicrystalline lamellar stacks. Qualitatively, it can be stated that the degree of crystal orientation in TPV materials increased with the thermoplast LDPE content, following the trend observed for the pure thermoplastic components.

The pure gluten rubber and TPV materials deformed homogeneously during tensile testing up to fracture. No necking was observed. As mentioned in section 3.2, the pure thermoplastic components displayed a faint yield point and necking. Figure 7 compares the mechanical properties of the TPVs with those of the pure components.

All TPV moduli were in between the values of the pure components (Figure 7A). Due to the large experimental errors, rationalizing the TPV moduli in terms of equations based on the phase volume fractions, the pure component moduli, a phase morphology dependent coupling mode and interfacial strengths (Dickie, 1978; Leclair and Favis, 1996), is not meaningful. Error bars for the Shore D hardness (Figure 7E) were smaller and the hardness could be computed from the rule of mixtures, i.e. the proportional sum of the pure component values. Such additivity represents a theoretical upper limit for the modulus of a phase separated blend and likely also for the hardness, given its qualitative relation with the modulus (Qi et al., 2003). However, in principle this limit cannot be obtained unless the component properties within the blend are different from those in the pure form (Kolarik, 1996; Wang et al., 2010). The rubber glycerol content in the TPVs was not different from that in the pure rubber and the gluten proteins in both materials display a minimal SDS extractability. A reduced crystallinity compared to that of the pure thermoplastic component can also be excluded since this would be expected to lower the hardness rather than to lift it to the upper limit. Although difficult to assess, an altered molecular orientation may have played a role (Figure 8). Applicability of the rule of mixtures for the modulus has been observed earlier in binary blends and was tentatively related to crystallization-induced matrix shrinkage, affecting the dispersed phases and the interfacial regions (Leclair and Favis, 1996).

Kolarik and Lednicky (1997) states that the rule of mixtures also represents the upper limit for the stress at break of binary (two-phase) blends and claims that any excess should be explained in terms of differences between the phases in the blend and the pure phases. The rule of mixtures could be used to accurately calculate the stress at break for the TPVs based on pure LDPE-g-MA and the 25/75 LDPE/LDPE-g-MA blend but the values of all other TPVs in Figure 7B exceeded the rule of mixture estimates. For these cases, the explanation is at least partially grounded in too low values for the stress at break of the pure thermoplastic components (the white bars in Figure 7B) on which the rule of mixture calculations are based. Recall that (faint) necking was observed and that none of the necks travelled

through the entire test specimen prior to failure. Premature failure at a defect naturally leads to too low, not representative stress at break values. For the rule of mixtures to hold for the LDPE and 75/25 LDPE/LDPE-g-MA based TPV materials, the stress at break for the pure thermoplastic components would have needed to increase by a factor of 1.5. This complication does not exist for the TPVs based on LDPE-g-MA and the 25/75 LDPE/LDPE-g-MA blend because failure of the pure thermoplastic systems happened without moving into a necking regime.

Applicability of the rule of mixtures in the latter cases suggests that there must be additional reasons for the excessively high stress at break values. Processing induced molecular orientation in the tensile direction might be one of them. However, since the TPVs rich in LDPE-g-MA hardly displayed any orientation (Figure 8), this is believed to be merely a secondary effect. The primary reason may well be related to TPV-typical mechanism of plastic deformation. Using in-situ atomic force microscopy during tensile testing Oderkerk et al. demonstrated for nylon-6/EPDM TPVs that the plastic deformation of the thermoplastic matrix phase is very heterogeneous even though the deformation macroscopically is homogeneous (Oderkerk et al., 2002). During straining, the plastic deformation is initiated in the thin matrix ligaments between the rubber particles at the rubber equatorial positions where the stress concentrates. Even at high strains, the (polar) thick ligaments of the matrix remain almost undeformed and act as adhesion points holding the rubber particles together. Figure 12(B) illustrates the deformed state with the plastically deformed matrix ligaments represented in black and the undeformed ones in white. As the material strain is realized by only a fraction of the matrix (together with the rubber particles) these deformed matrix ligaments locally experience a higher strain rate compared to what macroscopically is imposed. Higher strain rates lead to higher stresses in viscoelastic materials. In principle, deformation rate induced hardening may also apply to the rubbery phases and contribute to the observed high stress at break values. To our knowledge, no studies on the strain rate dependent deformation behavior of gluten rubbers have been reported to date. The slow (recovery) dynamics for gluten based rubbers suggest that this effect might be relevant.

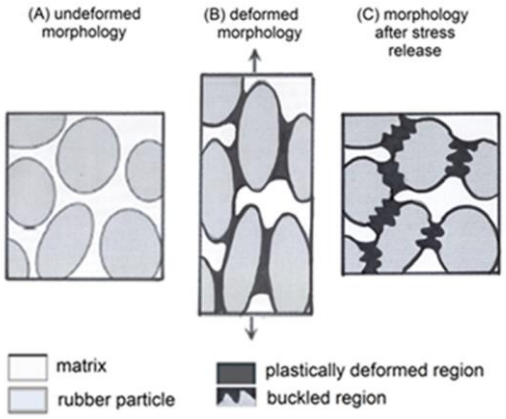

Fig. 12: TPV morphology at rest (A), during deformation in a tensile test (B) and recovered after stress release (C). The buckled regions in (C) represent the plastically deformed matrix ligaments that are pulled back by the rubber elastic forces.

Within experimental error, the rule of mixtures (incidentally) applied to the strain at break for the TPV based on the 25/75 LDPE/LDPE-g-MA blend (Figure 7C). All other values were much lower compared to additivity and below the pure component values. The very low strain at break for the TPV based on pure LDPE-g-MA strain most likely was related to its coarse phase morphology (Figure 9E). Because of this coarseness, the amount of thin matrix ligaments was rather low, leading to very localized stress concentrations. Excessive local plastic matrix deformation may have led to interfacial debonding and thus the initiation and propagation of voids with ultimately formation of catastrophic cracks. Finer morphologies, like those in Figure 12A, should delocalize the stress to a higher number of spots and should lead to improved ultimate strain values, which indeed was the case for the TPV based on the 25/75 LDPE/LDPE-g-MA blend. However, although the morphology became progressively finer with increasing LDPE fraction in the blend, a strong decrease of the strain at break is recorded. Obviously, the coarser morphology and the low interfacial strength for the TPV based on pure LDPE may have accounted for its poor performance. It is less clear why the TPVs based on the 75/25 and 50/50 LDPE/LDPE-g-MA behaved so badly, notwithstanding their fine morphology and strong interfaces, which should have postponed void formation. It is hard to verify whether or not the limited miscibility of LDPE with LDPE-g-MA contributed to the poor mechanical performance such as by the presence of weak interactions within the thermoplastic phase. Although this cannot be excluded, in the next paragraph, the thesis is defended that at least the starch and fibrous contaminations contribute to the low strain to failure values of these materials.

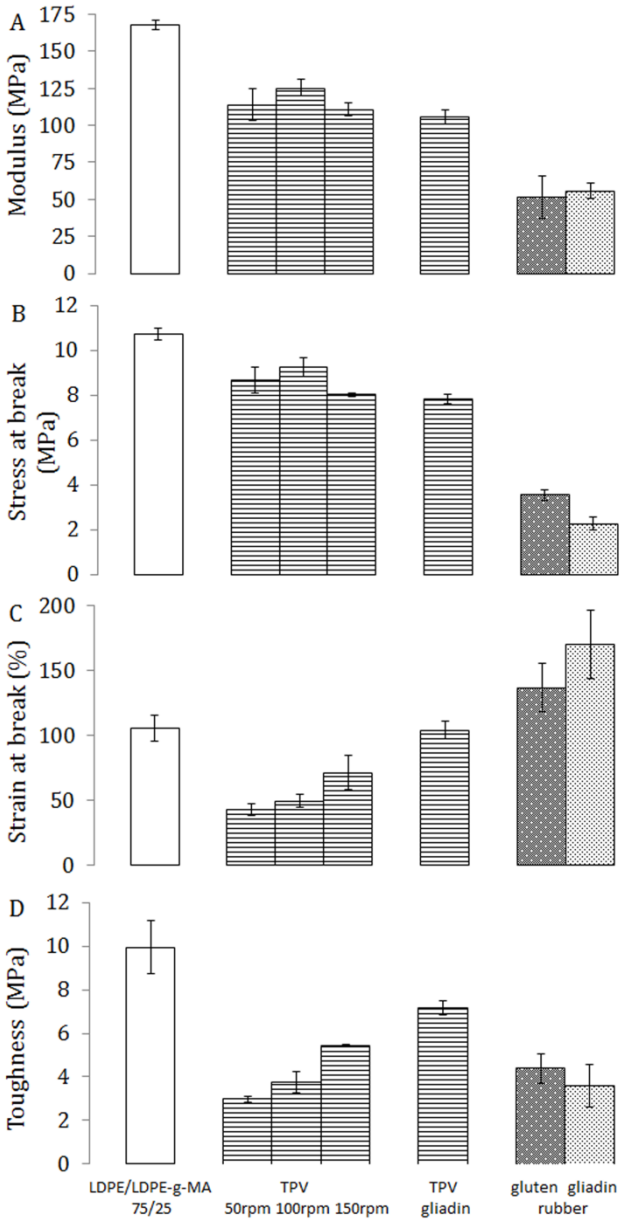

Fig. 13: Tensile test results for TPVs based on 40wt% 25/75 LDPE/LDPE-g-MA as matrix and 60 wt% rubber. The materials used for studying the variation in the extruder rotation speed (rpm) are based on gluten as rubber component. The gliadin based TPV was extruded at 100 rpm. For comparison the values of the pure rubbers (right side) and thermoplastic matrix (left side) are added. A: Young's modulus (MPa), B: stress at break (MPa), C: strain at break (%), D: toughness (MPa).

The plastic deformation in TPV materials is governed by the plastic deformation of the thermoplastic matrix phase (l'Abee et al., 2010). As long as the starch granules and fibrous materials are confined in the rubber phases, they are not expected to interfere with the matrix deformation processes. This is expected to be so for the coarse TPV morphologies with matrices rich in LDPE-g-MA. However, the contaminations are exposed to the matrix

provided the size of the rubber phases is comparable to or smaller than that of the contaminations, which is the case for TPV matrices rich in LDPE. The starch granules and fibrous contaminations were generally larger than 10 μm across whereas the rubber particles in e.g. the TPV based on the 75/25 LDPE/LDPE-g-MA blend were only about 2-3 μm in diameter (Figure 9B and 10D). Figures 4, 9 and 10 prove that the contaminations did not adhere well to the matrix or the rubber, implying that the continuous matrix network for LDPE rich TPVs was interrupted and that voids and catastrophic cracks are readily created.

It was demonstrated by means of microscopy (data not shown) that most of the contaminants were concentrated within the glutenin rich fraction during the gluten fractionation process. When using the gliadin enriched fraction as rubber component, the undesirable impact of contaminations was thus reduced. Indeed, the data in Figure 13 demonstrate that the strain at break increased up to the matrix value for a TPV based on 60 wt% gliadin rubber and 40 wt% of the 75/25 LDPE/LDPE-g-MA blend. Compared to its gluten rubber based counterpart (see the gluten TPV 100 rpm data in Figure 13), the modulus and stress at break of the gliadin rubber based TPV were slightly lower. All in all, the toughness of the gliadin based TPV was about twice as large as that of its gluten counterpart, essentially because of the higher strain to break of the former. The low toughness values for materials shown in Figure 7D were due to the low strains at break. The data on the gliadin rubber based TPV thus indicated that getting rid of contaminations is crucial for obtaining increased mechanical properties.

Figure 14A illustrates that by using the gliadin fraction a fine rubber dispersion was obtained with droplet sizes of about 2-3 μm in diameter. In fact, the droplet morphology for this TPV material is even clearer than in its gluten based counterpart (Figure 14C) prepared under similar conditions. The seemingly better developed morphology might be due to the fact that gliadin crosslinks at slightly higher temperatures than does glutenin (Lagrain at al., 2010) and to the lower average molecular weight of gliadin than that of full gluten. Both effects reduce the viscosity of the rubber precursor at the onset of the extrusion process by which smaller particles can be created prior to the morphological fixation by full crosslinking.

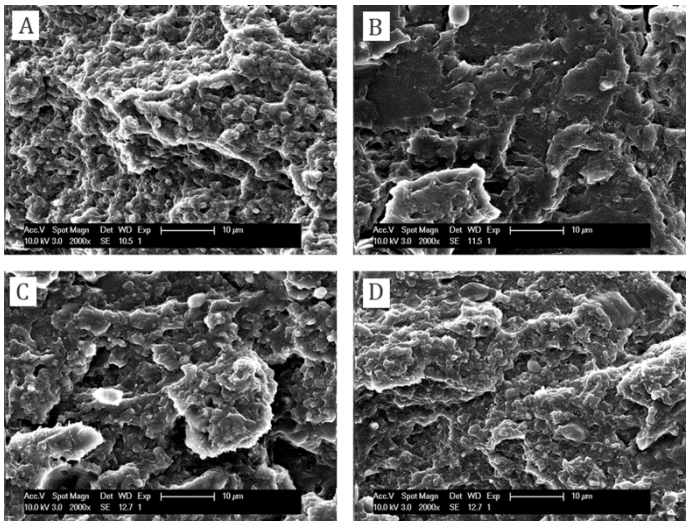

Fig. 14: SEM images of a TPV based on 60 wt% gliadin based rubber and 40 wt% 75/25 LDPE/LDPE-g-MA prepared using the extruder at 100 rpm for 5 min. B, C and D show morphologies of TPVs based on 60 wt% gluten based rubber and an identical thermoplastic matrix. The extruder was operated for 5 min at 50 rpm (B), 100 rpm (C) and 150 rpm (D). The surfaces were obtained by cryo-fracturing.

According to equation (1) finer dispersions can also be obtained by increasing the shear rate. Indeed, when the extruder was operated for 5 min at 50 rpm for a TPV based on 60 wt% gluten rubber and 40 wt% 75/25 LDPE/LDPE-g-MA, hardly any rubber particles could be seen. Figure 14B displays flake like features with a texture similar to that in Figure 4A, suggesting that at 50 rpm rather large rubber inclusions were obtained. The material properties were slightly inferior to those of the material prepared at 100 rpm (see Figure 13). The latter material held rather well dispersed rubber particles as illustrated in Figure 14C. With the extruder operated at 150 rpm an even better defined rubber particle dispersion was obtained (Figure 14D) with a morphology very similar to that in Figure 14A for the gliadin based TPV. The strain at break and the toughness of this 150 rpm material were superior to that of the material prepared at 100 rpm (see Figure 13). Better dispersions promote stress and strain delocalizations. The properties, however did not reach those of the 100 rpm gliadin rubber TPV likely because the latter contains less detrimental contaminations as discussed before.

3.3.2 About recyclability, reduced water absorption and recoverability

The goal of this research was to manufacture elastomeric materials based on wheat gluten without the disadvantages that thermosetting gluten rubbers have. This section highlights that the presented TPV materials are thermoplastic and absorb less water while maintaining the gluten rubber elasticity.

The thermoplastic character of the TPV materials obviously follows from the fact that they easily can be manufactured by extrusion and injection molding. However, the properties of the TPVs should be preserved even after many processing cycles for production scrap or waste material to be recyclable. Figure 15 shows the mechanical properties after multiple injection molding cycles for a material based on 60 wt% gluten rubber and 40 wt% 75/25

LDPE/LDPE-g-MA. Within experimental error, recycling this material 5 or 10 times did not alter the material properties compared to being injection molded only once. Figure 15 shows the properties of the once molded material (middle bar of the right side). Furthermore, no morphological changes could be observed by SEM and neither did the water absorption behavior or rubber like recovery alter by recycling (data not shown).

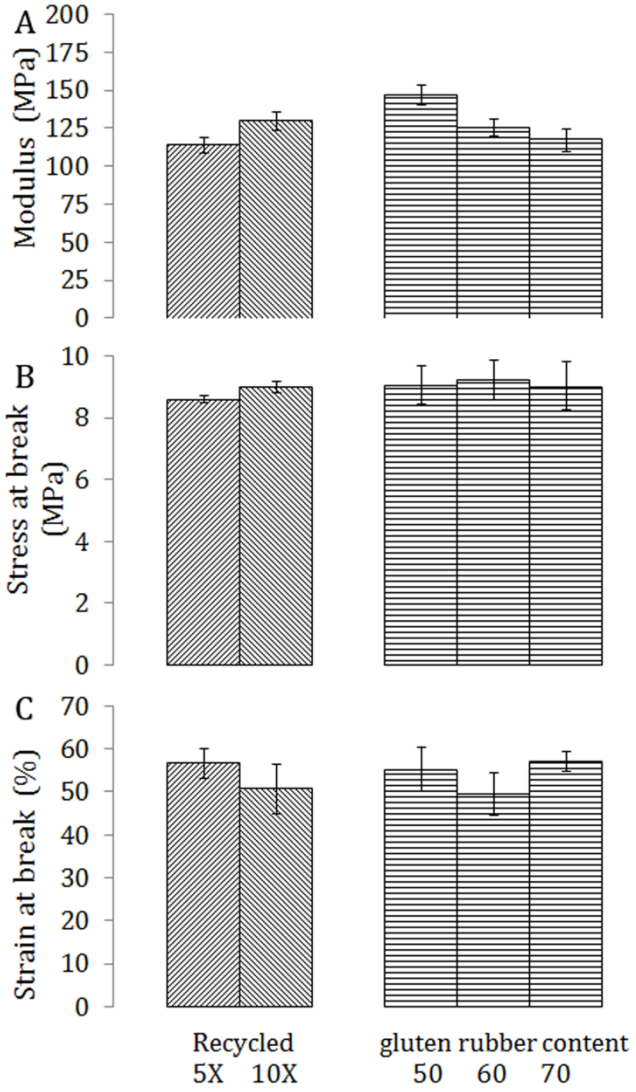

Fig. 15: Tensile test results on different TPV materials with (A) the modulus (0-2%), (B) the stress at break and (C) the strain at break. Left side bars: TPV materials based on 60 wt% gluten rubber and 40 wt% 75/25 LDPE/LDPE-g-MA prepared using the extruder at 100 rpm for 5 min. After the product was injection molded, it was granulated and injection molded (recycled) again for 5 or 10 times. Right side bars: injection molded TPV materials prepared using the extruder at 100 rpm for 5 min and based on 75/25 LDPE/LDPE-g-MA as matrix. Different gluten rubber contents are compared: 50, 60 and 70 wt%.

Figure 16 displays the time dependent rubber weight gain of the TPVs in water and compares it to that of pure gluten rubber. Pure 75/25 LDPE/LDPE-g-MA does not absorb

any water. To facilitate comparison with the pure rubber, the polyethylene mass was subtracted from the measured TPV weight and the remaining weight was normalized to the TPV gluten rubber fraction. In that way, the data in Figure 16 represent the weight gain of the rubber within the TPV materials, not that of the entire TPV. The dotted curve represents the rubber weight gain of the TPV based on 60 wt% gluten rubber and 40 wt% 75/25 LDPE/LDPE-g-MA, extruded at 100 rpm for 5 min and injection molded. Clearly, the TPV rubber weight gain evolves more slowly than in pure gluten rubber and did not surpass a maximum. The weight gain after about 100 hour was slightly higher than that of the pure rubber. Recall that the maximum was attributed to a combination of water uptake and glycerol release.

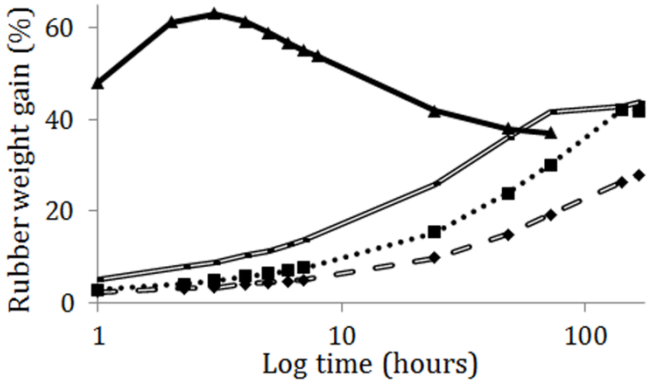

Fig. 16: Weight gain of the rubber fraction after submerging in water for TPVs based on 75/25 LDPE/LDPE-g-MA and 50 wt% (open dashed curve), 60 wt% (dotted curve) or 70 wt% (open line curve) gluten rubber. The water absorption behavior is compared to that of pure gluten rubber (full curve).

The absence of a maximum for the TPV rubber indicates either that both water uptake and glycerol release were retarded equally, such that a maximum would still have appeared after more than 100 hours submersion in water or that the processes more strongly overlapped such that the weight gain after about 100 hours arrived at approximately the same equilibrium as that of the pure gluten rubber without surpassing a maximum. The latter hypothesis evidently is wrong because drying the sample at 130°C and measuring the remaining weight revealed that only 35% of the glycerol has left the TPV at the end of the swelling experiment, instead of 80% for the pure gluten rubber material (cfr. supra). Altering the gluten rubber wt% provided further support for the first option. The final rubber weight gain for the TPV with 70 wt% rubber also overtook that of the pure rubber but seemed to level off. As there are no reasons for the TPV rubber to swell more strongly than the pure rubber, the leveling was interpreted as being due to reaching a maximum, rather than an equilibrium. In other words, more glycerol was expected to leave the sample at longer times.

Based on the time to reach the maximal weight gain, the 70% rubber TPV took up water / released glycerol about 100 times slower than pure gluten rubber. Secondly, the water uptake / glycerol release after a week of submersion was strongly reduced. The rate and uptake/release further reduced by lowering the rubber content within the TPV as

illustrated for the 50 wt% rubber TPV in Figure 16. That TPVs still exchanged solvents suggests that not all rubber inclusions were fully shielded from the environment by polyethylene. For high rubber fractions in particular, the morphology may have been partially co-continuous or part of the dispersed rubber phases may have made up a solvent accessible, interconnected network. Be that as it may, for some applications it might be sufficient that the water uptake of all studied TPVs after 1 hour submersion is vanishingly small compared to that of pure gluten rubber. In water vapor conditions, this difference might even be more outspoken.

Figure 15 illustrates that tensile properties did not strongly depend on the rubber fraction over the range studied. Only the modulus followed the polyethylene fraction.

Given the low strain at break values for the TPV materials, recovery testing was limited to rather small upper strains of about 10%. Figure 17 displays the stress recorded during stretching and subsequent strain inversion for the TPV based on 60 wt% gluten rubber and 40 wt% 75/25 LDPE/LDPE-g-MA. The recovery under the present conditions equaled 80% and thus that of the pure gluten rubber and pure thermoplastic material, of which the recovery experiments are also shown in Figure 17. Figure 12C illustrates the key mechanism believed to be responsible for the elastic behavior of TPVs. When the external force is removed or reduced, the elastic forces of the stretched, dispersed rubber phases pull back the plastically deformed matrix parts by either buckling or bending (Oderkerk et al., 2002; Paul, 1978). Most likely this mechanism applies here as well, although this cannot be easily derived from the recovery experiments, since the separate components recovered equally well as the TPV. A good recovery is no surprise for the gluten rubber. The high polyethylene recovery undoubtedly results from the fact that straining was limited to below the onset of necking (which occurs at 10-15 % strain). Stretching the matrix component beyond its necking regime would surely limit the recovery. Given the stress localization in the TPV materials, local matrix yielding should have occurred and therefore recovery should have been assisted by the rubber elastic forces. That the stresses in a second recovery cycle on the same sample were reduced, supports this idea (data not shown). The softening upon reloading can be explained by the fact that the thinnest parts of the matrix had already been plastically deformed and only had to be unfolded during the start of the second deformation, which required significantly less force (Boyce et al., 2001b).

TPV materials based on the same 75/25 LDPE/LDPE-g-MA matrix that were processed at 150 rpm or that contain 50 or 70 wt% gluten rubber recovered equally well under identical conditions.

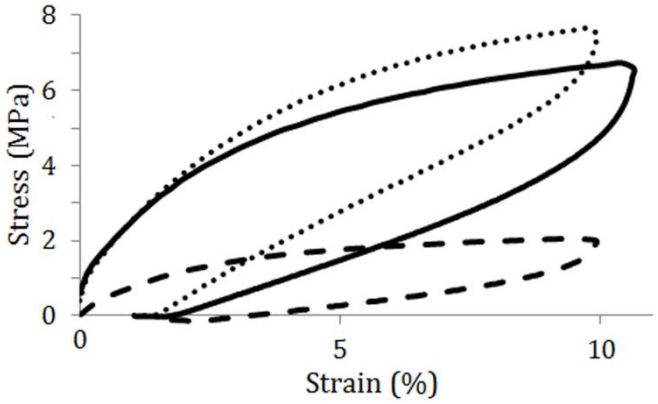

Fig. 17: Strain recovery curves for the TPV with 60 wt% gluten rubber and 40 wt% 75/25 LDPE/LDPE-g-MA extruded at 100 rpm (full line) compared to its pure components: 25/75 LDPE/LDPE-g-MA (dotted line) and pure gluten rubber (dashed line).

4. Conclusions

The goal of this research was to develop wheat gluten based thermoplastic elastomers with a reduced tendency to absorb water but with elastomeric properties comparable to those of existing, medium hard, thermosetting rubbers made from wheat gluten and glycerol as plasticizer. Taking advantage of the fact that gluten crosslinks at high temperatures, thermoplastic vulcanisates (TPVs) were prepared by extruding a glycerol plasticized gluten rubber precursor at 130°C in presence of thermoplastic LDPE to which LDPE-g-MA was added. A blend consisting of 75 wt% LDPE and 25 wt% LDPE-g-MA seemed to be a good compromise in which the LDPE high molecular weight as well as the LDPE-g-MA compatibilizing action were exploited to reach a phase-separated morphology composed of finely dispersed gluten rubber particles with interfaces covalently anchored to a thermoplastic matrix. TPVs were manufactured which contained up to 70 wt% gluten rubber. Protein extractability experiments combined with SE-HPLC revealed that the gluten precursor indeed crosslinked during extrusion and that thermal degradation was limited. Furthermore, no glycerol was lost during the extrusion process.

Given the thermoplastic matrix, the entire material is thermoplastic and can be injection molded multiple times without losing mechanical performance. Because of the hydrophobic thermoplastic matrix, the water absorption and glycerol leaching when submerged in water were 100 times slower compared to in classical gluten rubber materials. The TPV water uptake after 1 hour was negligibly small and decreased with the gluten rubber content in the TPV materials. At the low strain levels studied, the TPV recovery after mechanical loading was identical to that of pure gluten rubber.

The TPV tensile modulus and stress at break values were rather high when compared to the pure component values. The high stress values were tentatively associated with the TPV-typical heterogeneous, plastic deformation, involving locally rather high strain rates when compared to the macroscopically imposed strain rate. The low strains at break - even for optimized TPVs with finely dispersed rubber particles - was related to a combination of two factors: the limited miscibility of LDPE with LDPE-g-MA and the presence of starch and fibrous contaminations, which did adhere well neither to the matrix not to the rubber.

These contaminants were exposed to the matrix when the size of the rubber phases was comparable to or smaller than that of the contaminations, resulting readily in voids and catastrophic cracks upon deformation. The latter hypothesis was supported by experiments in which a gliadin enriched fraction was used for the manufacturing of the rubber component. This fraction is relatively free from contaminants and as a result the corresponding TPV strain at break increased up to the matrix value.

Wheat gluten based thermoplastic vulcanizates were thus successfully prepared and may represent a (partially) bio-based alternative for thermoplastic elastomers from fossil resources at suitable temperature and humidity conditions.

Acknowledgements

The authors wish to acknowledge the Agency for Innovation through Science and Technology Flanders (IWT Vlaanderen) and the KU Leuven Industrial research fund for financial support. B. Goderis thanks the Hercules Foundation for supporting the purchase of equipment (AKUL/09/0035, Molybdenum high-energy X-ray source for in situ diffraction studies of advanced materials and single crystals). Jan A. Delcour is W.K. Kellogg Chair of Cereal Science and Nutrition at KU Leuven. Ignaas Verpoest is Toray Chair in Composite Materials at KU Leuven

References

AbdouSabet, S. and Puydak, R. and Rader, C. Dynamically vulcanized thermoplastic elastomers, Rubber Chemistry and Technology 69 (3) (1996) 476-494, doi: 10.5254/1.3538382

Babu, K. and Naskar, R. Recent developments on thermoplastic elastomers by dynamic vulcanization, Advanced Polymer Science 239 (2011) 219-248, doi: 10.1007/12_2010_97

Babu, R. and O'Connor, K. and Seeram, R. Current progress on bio-based polymers and their future trends, Progress in Biomaterials 2 (2013) 8, doi: 10.1186/2194-0517-2-8

Bietz, J. and Lookhart, G. Properties and non-food potential of gluten, Cereal Foods World 41 (1996) 376-382.

Bikiaris, D. and Prinos, J. and Koutsopoulos, K. and Vouroutzis, N. and Pavlidou, E. and Frangis, N. and Panayiotou, C. LDPE/plasticized starch blends containing PE-g-MA copolymer as compatibilizer, Polymer degradation and stability 59 (1-3) (1998) 287-291, Symposium on Biodegradable Polymers and Macromolecules, at the E-MRS 97/ICAM 97 Conference, Strasbourg, France, Jun 16-19, 1997, doi: 10.1016/S0141-3910(97)00126-2

Borah, J.S. and Chaki, T.K. Thermogravimetric and dynamic mechanical analysis of LLDPE/EMA blends, Journal of Thermal Analysis and Calorimetry 105 (1) (2011) 365-373, doi: 10.1007/s10973-011-1489-6

Boyce, M. and Socrate, S. and Kear, K. and Yeh, O. and Shaw, K. Micromechanisms of deformation and recovery in thermoplastic vulcanizates, Journal of the Mechanics and Physics of Solids 49 (6) (2001a) 1323-1342

Boyce, M. and Yeh, O. and Socrate, S. and Kear, K. and Shaw, K. Micromechanics of cyclic softening in thermoplastic vulcanizates, Journal of the Mechanics and Physics of Solids 49 (6) (2001b) 1343-1360, doi: 10.1016/S0022-5096(00)00077-6

Castello, M. and Dweck, J. and Aranda, D. Thermal stability and water content determination of glycerol by thermogravimetry, Journal of Thermal Analysis and Calorimetry 97 (2009) 627-630, doi: 10.1007/s10973-009-0070-z

Coran, A. and Patel, R. Rubber thermoplastic compositions 4. Thermoplastic vulcanizates from various rubber plastic combinations, Rubber Chemistry and Technology 54 (4) (1981) 892-903, doi: 10.5254/1.3535842

Day, L. and Augustin, M. and Batey, I. and Wrigley, C. Wheat-gluten uses and industry needs, Trends in Food Science & Technology 17 (2) (2006) 82-90, doi: 10.1016/j.tifs.2005.10.003

Delcour, J.A. and Hoseney, R. Principles of cereal science and technology, third edition, AACC International Inc. (2010), doi: 10.1146/annurev-food-022811-101303

Delcour, J.A. and Joye, I.J. and Pareyt, B. and Wilderjans, E. and Brijs, K. and Lagrain, B. Wheat Gluten Functionality as a Quality Determinant in Cereal-Based Food Products, in: Doyle, MP and Klaenhammer, TR (Ed.), Annual review of food science and technology, 3 (2012), doi: 10.1146/annurev-food-022811-101303

Dickie, R.A. Polymer Blends Chapter 8, Academic Press Inc., New York, 1978

Domenek, S. and Feuilloley, P. and Gratraud, J. and Morel, M. and Guilbert, S. Biodegradability of wheat gluten based bioplastics, Chemosphere 54 (4) (2004) 551-559, doi: 10.1016/S0045-6535(03)00760-4

Fernandes, P. and Ramos, M. Theoretical insights into the mechanism for thiol/disulfide exchange, Chemistry a European Journal 10 (1) (2004) 257-266, doi: 10.1002/chem.200305343

Gessler, A. and Haslett, W. Process for preparing a vulcanized blend of crystalline polypropylene and chlorinated butyl rubber, US patent (1962) 3 037 954, 1962.49

Gomez-Martinez, D. and Barneto, A.G. and Martinez, I. and Partal, P. Modelling of pyrolysis and combustion of gluten-glycerol-based bioplastics, Bioresource Technology 102 (10) (2011) 6246-6253, doi: 10.1016/j.biortech.2011.02.074

Grace, H. Dispersion Phenomena in high viscosity immiscible fluid systems and application of static mixers as dispersion devices in such systems, Chemical engineering communications 14 (3-6) (1982) 225-277, doi: 10.1080/00986448208911047

Heeley, E.L. and Gough, T. and Hughes, D.J. and Bras, W. and Rieger, J. and Ryan, A. J. Effect of processing parameters on the morphology development during extrusion of polyethylene tape: an in-line small-angle X-ray scattering (SAXS) study, Polymer 54 (2013) 6580-6588, doi: 10.1016/j.polymer.2013.10.004

Huang, J. and Keskkula, H. and Paul, D. Elastomer particle morphology in ternary blends of mealeated and non-maleated ethylene-based elastomers with polyamides: Role of elastomer phase miscibility., Polymer 47 (2006) 624-638, doi: 10.1016/j.polymer.2005.11.087

Jansens, K.J.A. and Lagrain, B. and Rombouts, I. and Brijs, K. and Smet, M. and Delcour, J.A. Effect of temperature, time and wheat gluten moisture content on wheat gluten network formation during thermomolding, Journal of Cereal Science 54 (3) (2011) 434-441, doi: 10.1016/j.jcs.2011.08.008

Jansens, K.J.A. and Vo Hong, N. and Telen, L. and Brijs, K. and Lagrain, B. and Van Vuure, A. and Van Acker, K. and Verpoest, I. and Van Puyvelde, P. and Goderis, B. and Smet, M. and Delcour, J.A. Effect of molding conditions and moisture content on the mechanical properties of compression molded glass, wheat gluten bio-plastics., Industrial Crops and Products 44 (2013) 480-487, doi: 10.1016/j.indcrop.2012.10.006

Jiang, C.H. and Filippi, S. and Magagnini, P. Reactive compatibilizer precursors for LDPE/PA6 blends. II: maleic anhydride grafted polyethylenes, Polymer 44 (8) (2003) 2411-2422, doi: 10.1016/S0032-3861(03)00133-2

Kolarik, J. Simultaneous prediction of the modulus and yield strength of binary polymer blends, Polymer Engineering and Science 36 (1996) 2518-2524, doi: 10.1002/pen.10650

Kolarik, J. and Lednicky, F. Ultimate properties of polycarbonate blends: effects of inclusion plastic deformation and of matrix phase continuity, Polymer Engineering and Science 37 (1997) 128-137, doi: 10.1002/pen.11653

l'Abee, R.M.A. and Van Duin, M. and Spoelstra, A.B. and Goosens, J.G.P. The rubber particle size to control the properties-processing balance of thermoplastic/cross-linked elastomer blends, Soft Matter 6 (2010) 1758-1768, doi: 10.1039/B913458A

Lagrain, B. and Brijs, K. and Veraverbeke, W. and Delcour, J.A. The impact of heating and cooling on the physico-chemical properties of wheat gluten-water suspensions, Journal of CerealScience 42 (3) (2005) 327-333, doi: 10.1016/j.jcs.2005.06.005

Lagrain, B. and Goderis, B. and Brijs, K. and Delcour, J.A. Molecular Basis of Processing Wheat Gluten toward Biobased Materials, Biomacromolecules 11 (3) (2010) 533-541, doi: 10.1021/bm100008p

Leclair, A. and Favis, B.D. The role of interfacial contact in immiscible binary polymer blends and its influence on mechanical properties, Polymer 37 (1996) 4723-4728, doi: 10.1016/S0032-3861(96)00319-9

Mathot, V.B.F. Temperature dependence of some thermodynamic functions for amorphous and semicrystalline Polymers, Polymer 25 (1984) 579-599, doi: 10.1016/0032-3861(84)90025-9

Mathot, V.B.F. Calorimetry and Thermal Analysis of Polymers, Hanser Publishers, New York (1994), doi: 10.1002/pi.1995.210370112

Moly, K. and Bhagawan, S. and Groeninckx, G. and Thomas, S. Correlation between the morphology and dynamic mechanical properties of ethylene vinylacetate/linear low-density polyethylene blends: Effects of the blend ratio and compatibilization, Journal of Applied Polymer Science 100 (6) (2006) 4526-4538, doi: 10.1002/app.22466

Oderkerk, J. and de Schaetzen, G. and Goderis, B. and Hellemans, L. and Groeninckx, G. Micromechanical deformation and recovery processes of nylon-6 rubber thermoplastic

vulcanizates as studied by atomic force microscopy and transmission electron microscopy, Macromolecules 35 (17) (2002) 6623-6629, doi: 10.1021/ma0113475

Paul, D. Polymer blends, Academic press New York, 1978.

Redl, A. and Guilbert, S. and Morel, M. Heat and shear mediated polymerisation of plasticized wheat gluten protein upon mixing, Journal of Cereal Science 38 (1) (2003) 105-114, doi: 10.1016/S0733-5210(03)00003-1

Pommet, M. and Redl, A. and Guilbert, S. and Morel, M. Intrinsic influence of various plasticizers on functional properties and reactivity of wheat gluten thermoplastic materials, Journal of Cereal Science 42 (1) (2005) 81-91, doi: 10.1016/j.jcs.2005.02.005

Qi, H.J. and Joyce, K. and Boyce, M.C. Durometer hardness and the stress-strain behavior of elastomeric materials, Rubber Chemistry and Technology 76 (2003) 419-435, doi: 10.5254/1.3547752

Rombouts, I. and Lamberts, L. and Celus, I. and Lagrain, B. and Brijs, K. and Delcour, J.A. Wheat gluten amino acid composition analysis by high-performance anion-exchange chromatography with integrated pulsed amperometric detection, Journal of Chromatography A 1216 (29) (2009) 5557-5562, doi: 10.1016/j.chroma.2009.05.066

Schofield, J. and Bottomley, R. and Timms, M. and Booth, M. The effect of heat on wheat gluten and the involvement of sulfhydryl disulfide interchange reactions, Journal of Cereal Science 1 (4) (1983) 241-253, doi: 10.1016/S0733-5210(83)80012-5

Sun, S. and Song, Y. and Zheng, Q. Morphologies and properties of thermo-molded biodegradable plastics based on glycerol-plasticized wheat gluten, Food Hydrocolloids 21 (7) (2007) 1005-1013, doi: 10.1016/j.foodhyd.2006.03.004

Sun, S. and Song, Y. and Zheng, Q. Thermo-molded wheat gluten plastics plasticized with glycerol: Effect of molding temperature, Food hydrocolloids 22 (6) (2008a) 1006-1013, doi: 10.1016/j.foodhyd.2007.05.012

Sun, S. and Song, Y. and Zheng, Q. Morphology and mechanical properties of thermo-molded bioplastics based on glycerol-plasticized wheat gliadins., Journal of Cereal Science 48 (2008b) 613-618, doi: 10.1016/j.jcs.2008.01.005

Taylor, G. The viscosity of a fluid containing small drops of another fluid, Proceedings of the Royal Society of London A 138 (1932) 41–48, doi: 10.1098/rspa.1932.0169

Utracki, L.A. Polymer Alloys and Blends, Hanser Publishers, Munich (1990)

Van Der Borght, A. and Goesaert, H. and Veraverbeke, W.S. and Delcour, J.A. Fractionation of wheat and wheat our into starch and gluten: overview of the main processes and the factors involved, Journal of Cereal Science 41 (3) (2005) 221-237, doi: 10.1016/j.jcs.2004.09.008

Veraverbeke, W.S. and Delcour, J.A. Wheat protein composition and properties of wheat glutenin in relation to breadmaking functionality, Critical Reviews in Food Science and Nutrition 42 (3) (2002) 179-208, doi: 10.1080/10408690290825510

Wang, S. and Sue, H. and Jane, J. Effects of polyhydric alcohols on the mechanical properties of soy protein plastics., Journal of Macromolecular Science, Part A: Pure and Applied Chemistry 33 (1996) 557-569, doi: 10.1080/10601329608010878

Wang, J.F. and Carson, J.K. and North, M.F. and Cleland, D.J.A knotted and interconnected skeleton structural model for predicting Young's modulus of binary phase polymer blends, Polymer Engineering and Science 50 (2010) 643-651, doi: 10.1002/pen.21592

Wang, Z. and Wang, L. and Wang, X. and Hao, C. Deformation reversibility enhancement of thermoplastic vulcanizates based on high density polyethylene and ethylene-propylene-diene terpolymer, Materials Chemistry and Physics 134 (2012) 1185-1189, doi: 10.1016/j.matchemphys.2012.04.019